IOP Conf. Series: Materials Science and Engineering **219** (2017) 012040 doi:10.1088/1757-899X/219/1/012040

Effect of strain-path change on the anisotropic mechanical properties of a commercially pure aluminum

P L Sun[1,*] and S J Huang[2]

[1]Department of Materials and Optoelectronic Science, National Sun Yat-sen University, Kaohsiung 80424, Taiwan
[2]Department of Materials Science and Engineering, Feng Chia University, Taichung 40724, Taiwan

Email address: plsun@mail.nsysu.edu.tw

Abstract. Samples of commercially pure aluminum were subjected to equal channel angular extrusion (ECAE) using a 90° square die by routes A and C, where the specimens are not rotated and are rotated 180° between extrusion passes, respectively. Qualitatively similar anisotropic responses under compressive loading along the three orthogonal directions of the ECAE billet are seen in both cases. The plastic anisotropy is related to the effect of strain-path change, namely that different slip activities are induced for specimens loaded along different directions with respect to the last ECAE pass. The anisotropic mechanical behavior is more evident in the sample deformed by route C. Considering the shear patterns imposed in each ECAE route, the characteristics of dislocations introduced in ECAE should affect the mechanical response in post-ECAE loading. It is suggested that during the ECAE process, dislocations on fewer slip systems are activated in route C than in route A, and therefore, a stronger plastic anisotropy results in this sample. The as-ECAE specimens were also heat treated to achieve a recovery-annealed state. The plastic anisotropy persists in the annealed specimens to slightly reduced extent, which can be ascribed to partial annihilation of pre-existing dislocations.

1. Introduction

It has been well established in the past two decades that metals with ultrafine-grained (UFG) structures can be generated by the use of equal channel angular extrusion (ECAE) [1-3]. After processing by ECAE at ambient temperature, the microstructures of most alloys are quite complex. The morphology of the subgrains/grains constituting the microstructure may vary from lamellar to polyhedral shape [3-5]. The boundaries separating neighboring subgrains/grains are mixtures of segments with misorientation angles ranging from low to high angles, and the boundary structure can vary from dislocation walls (DW), to partially transformed boundaries (PTB) and to grain boundaries (GB) [4]. It was found that low temperature annealing can be applied to slightly tailor the grain size and boundary structure of UFG metals produced by ECAE, in which annealing is carried out at a temperature below the onset of recrystallization [6, 7].

According to Yu *et al*. [8], an evident transition of tensile behavior appears as the grain size is reduced from the micrometer to submicrometer range in aluminum. It was proposed that as the grain size decreases below a critical value, which may correspond to the cell size, the mean free path of dislocations is no longer determined by the dislocation structure, but is limited by the grain boundaries

[8-11]. This causes an enhancement of dynamic recovery as well as a reduction of work hardening in UFG metals, and consequently leads to reduced tensile elongation [8]. The boundary structure was shown to play an important role in the tensile behavior of UFG aluminum [12]. Quasistatic tests revealed an increase in ductility with an increase in the percentage of low-angle boundaries [12].

In the ECAE process metals are deformed via a nearly simple shear [13], which imparts substantial texture and microstructure evolution. In multiple ECAE passes, the processing route and number of passes influence the microstructure and texture development, and thus affect the mechanical properties of the product. Anisotropy in initial flow stress and work-hardening have been reported in metals deformed by ECAE [14-20]. As the last pass in the process of multiple-pass ECAE treatments is believed to be most influential on properties of the processed materials, a knowledge of the anisotropic properties of materials processed by single-pass ECAE should facilitate the understanding of multi-passed materials. Work done on the anisotropic mechanical properties of aluminum processed by ECAE has mainly been focused on that deformed by single pass ECAE, while relatively little work has been done on aluminum processed by multiple pass ECAE [18-20]. The work of Haouaoui *et al*. [14] reveals that copper subjected to only one ECAE pass can result in both tensile and compressive yield stresses decreasing following the order of along Y-axis (perpendicular to the flow plane) > along Z-axis (normal to the top surface at the point of exit) > along X-axis (the extrusion direction). Strain-path change (SPC) is involved in uniaxial tension or compression tests of materials pre-deformed by ECAE. According to Li [17], SPC is an important factor, in addition to texture, to be considered in interpreting the plastic responses of ECAE processed metals subjected to uniaxial loading.

Compared to single-pass ECAE-processed materials, multiple-pass processed counterparts are expected to possess quite different texture and microstructure, which may be strongly affected by material, die angle, processing route, and number of passes used in the deformation process. Horita *et al*. [18] used AA1100 commercially pure aluminum, deformed by ECAE route Bc for 6 passes, and the yield stress decreased following the order of X-axis > Y-axis > Z-axis. Beyerlein *et al*. [19] employed oxygen-free pure copper and pure aluminum to study the anisotropic mechanical behavior of the as-ECAE samples, and found that the order of flow stresses among the three directions evolves similarly with pass number in the two materials. After the first pass, it is in the order of Y-axis > Z-axis > X-axis and after subsequent passes, Y-axis > X-axis ≈ Z-axis. It should be noted that single-pass processed materials was considered as plastically deformed *coarse-grained materials*, while multi-pass processed materials have *UFG structures*, which may behave quite differently from coarse-grained materials.

This work aims at understanding the anisotropic mechanical behavior of UFG aluminum produced by ECAE. Samples of commercial purity aluminum processed by ECAE routes A and C were investigated, both in the as-ECAE state and in a low temperature annealed state. The microstructures produced by ECAE routes A and C are distinctly different because these two routes provide plastic deformation via different shear patterns [21]. In particular, aluminum processed by ECAE route A possesses higher proportion of high angle boundaries (HABs) than route C (67% versus 35% [22]), which has been shown to play an important role in tensile behavior of UFG aluminum [12]. Therefore, a comparison between aluminum processed by ECAE routes A and C should improve our understanding of the effect of boundary structure on the anisotropic mechanical responses of UFG aluminum. Moreover, most of the studies reported in the literature on the anisotropic properties of ECAE metals are focused on the as-ECAE condition. A direct comparison between the results of a recovery annealed and as-ECAE counterpart can help to elucidate the influence of the residual dislocations on the anisotropic mechanical response of ECAE processed aluminum.

2. Experimental

A sample of commercially pure aluminum, AA1050, was homogenized at 873 K for 12 hours and slowly cooled to room temperature in air. The resulting average grain size was 330 μm. Rectangular billets were used for ECAE process. Billets were then subjected to ECAE route A or route C in a 90° square die. Billets were subjected to eight passes, giving an accumulated von Mises strain of ≈ 8.4. All

extrusions were performed at room temperature. A detailed description of the ECAE processing used for these samples can be found in a previous paper [3]. Recovery annealing was conducted at 523 K for 1 hour after ECAE. In the following text, **A** and **C** will refer to samples processed by route A and route C in the as-ECAE state, respectively, while the annealed counterparts will be denoted as AR and CR. The ECAE extrusion direction is defined as the *X*-axis, the flow plane normal is designated as the *Y*-axis, and the *Z*-axis is normal to both the *X*- and *Y*-axes.

The grain size of the specimens was measured on thin foils sectioned from all three orthogonal planes (the *X*-, *Y*, and *Z*-planes) using a transmission electron microscope (TEM) (Philips CM200) operated at 200 kV. The grain size of each grain is defined as the diameter of an equivalent circle with the same area as the grain. Additionally, due to the formation of elongated grains after ECAE, the grain shape was described by its length and width. Ellipses were used to fit every grain. The lengths of the long and short axes of the best fitting ellipse represent the grain length and width, respectively.

Samples for compression tests were sectioned to have dimensions of $6 \times 4 \times 4$ mm^3 from the center of the as-ECAE billets, in which the long axis was parallel to the loading direction (either the *X*-, *Y*- or *Z*-axis). Samples were ground and polished to have smooth surfaces prior to compression testing. Compression tests along all three loading directions were conducted at an initial strain rate of 7.1×10^{-4} s^{-1} at room temperature by using an Instron 5582 universal testing machine. Duplicate tests were conducted for all conditions to assure reproducibility. The sample surfaces were observed in a stereomicroscope and a HITACHI S3000 scanning electron microscope (SEM) at 15 kV after compression testing.

3. Results

3.1. Microstructure

The boundary character and texture of the same material after processing by ECAE route A and C for 8 passes have been reported in previous papers [3, 22]. The microstructural characteristics of the A and C specimens are summarized here. The texture of the as-ECAE specimen was observed to persist after annealing up to grain sizes greater than 10 μm in this material [6]. Therefore, the texture of the annealed specimens (AR and CR) is believed to be similar to that of the as-ECAE counterpart. Aluminum processed by 8 ECAE passes with either route A or route C exhibits similar crystallographic texture [22], which has the same characteristics of single-pass processed aluminum [23]. Texture strengths calculated from orientation distribution functions (ODFs) for A and C are 1.58 and 1.38, respectively, implying moderately weak textures [22, 24].

High angle boundaries are defined as boundaries with misorientation angles greater than 15° while low angle boundaries (LABs) have misorientation angles smaller than 15°. The aluminum processed by ECAE route A possesses higher proportion of HABs than route C (67% versus 35% [3, 22]). The experimental results from our previous work indicate that the ECAE samples annealed at 523K for 4 hours show similar proportion of HABs to that of the as-ECAE state [6]. Therefore, this indicates that the HAB% remains unchanged in both A and C specimens after annealed at 523K for one hour.

The microstructures of A, C, AR and CR were examined on the three orthogonal planes by using TEM and the results are given in figures 1-3. The quantitative results of the grain size and shape are summarized in table 1. Grains in specimen A exhibit mainly elongated shape on the *X*- or *Y*-plane but roughly equiaxed shape on the *Z*-plane. Based on the grain morphology on the three orthogonal planes, the grains in sample A can be considered as pancake (or disc) shape with the face approximately parallel to the *Z*-plane. The majority of grains in sample C are roughly equiaxed (aspect ratio ~ 2) on all three planes (table 1). The grains in sample A were measured to be slightly smaller than those in sample C. In both samples A and C, obvious diffraction contrast variation appears within the grain interior, which indicates the presence of considerable amount of defects and internal stresses in the as-ECAE condition (figure 1).

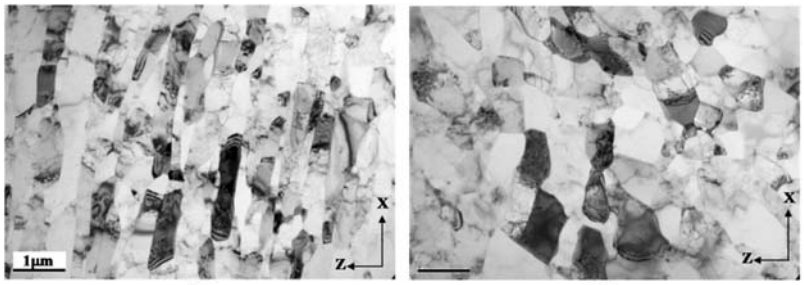

Figure 1. TEM micrographs of (a) specimen A and (b) specimen C on the Y-plane.

Figure 2. TEM micrographs on the (a) X, (b) Y and (c) Z planes for the AR specimen.

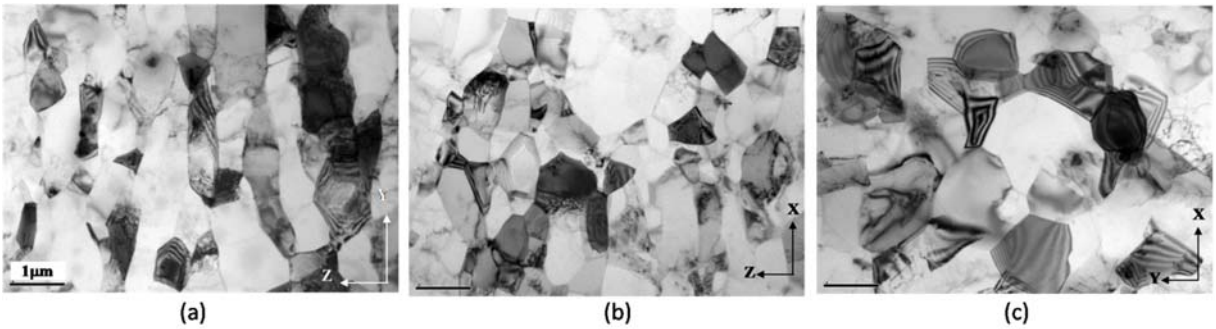

Figure 3. TEM micrographs on the (a) X, (b) Y and (c) Z planes for the CR specimen.

Table 1. Quantitative microstructural parameters obtained from measurements on the three *orthogonal* planes for each sample.

material	X-plane		Y-plane		Z-plane		D (μm)
	d_X (μm)	R_X	d_Y (μm)	R_Y	d_Z (μm)	R_Z	
A	0.54±0.21 [3]	2.56	0.56±0.26 [3]	2.71	0.68±0.39	1.82	0.59
C	0.68±0.29 [3]	2.08	0.61±0.30 [3]	1.89	0.70±0.40	1.67	0.66
AR	0.64±0.28	1.90	0.64±0.25	1.92	0.94±0.44	1.53	0.73
CR	0.76±0.38	2.00	0.71±0.38	1.68	0.94±0.45	1.56	0.80

*$D = (d_X d_Y d_Z)^{1/3}$, where d_X, d_Y, and d_Z are grain sizes measured on the three orthogonal planes. Grain size is defined as the equivalent circle diameter. Grain aspect ratio, R, is defined as the ratio of grain length over width.

After annealing, the grain structures in the AR and CR are more comparable, in which the majority of grains in both specimens have equiaxed shape (figures 2 and 3). The average grain size in sample CR is slightly larger than that in sample AR (table 1). As compared to samples A and C, the diffraction contrast in samples AR and CR is more uniform, indicating defect density and internal

stresses are substantially reduced. Additionally, most of the grains in samples AR and CR are enclosed by boundaries with clear grain boundary fringes (figures 2 and 3).

3.2. Compression tests

The true stress-strain curves obtained from compression tests along three loading directions of the specimens are presented in figure 4. The results indicate that specimen A has higher yield stress and flow stress than specimen C in all three loading directions. Compressive yield stresses along the three loading directions are found to be follow the order of Y-axis > *Z*-axis > *X*-axis in both the A and C specimens, and the differences in yield stresses are observed to be more significant in sample C than in sample A. The as-ECAE specimens exhibit slight work-softening when testing in both the X- and Y-directions, but slight hardening in the Z-direction.

The annealed samples, AR and CR, show reduced yield and flow stresses as compared to the as-ECAE counterparts (figure 4). Similar to the as-ECAE samples, specimen AR has higher yield stress and flow stress than specimen CR due to the smaller grain size and higher fraction of HABs in the AR specimen. The flow curves of the AR specimen display the "yielding peak" phenomenon in all three loading directions. On the other hand, the yielding peak is less evident in specimen CR, and can only be observed in the Y-direction. Yield stresses along the three loading directions are determined to follow the order of *Y*-axis > *Z*-axis > *X*-axis in specimen AR, while they follow the order of *Y*-axis ≈ *Z*-axis > *X*-axis in specimen CR. The differences in yield/flow stress become less significant in the annealed specimens as compared to their as-deformed states. A "yielding peak" only occurs in the annealed state, and is more evident in the AR sample than in the CR sample. In terms of loading direction, it is most apparent in the Y-direction.

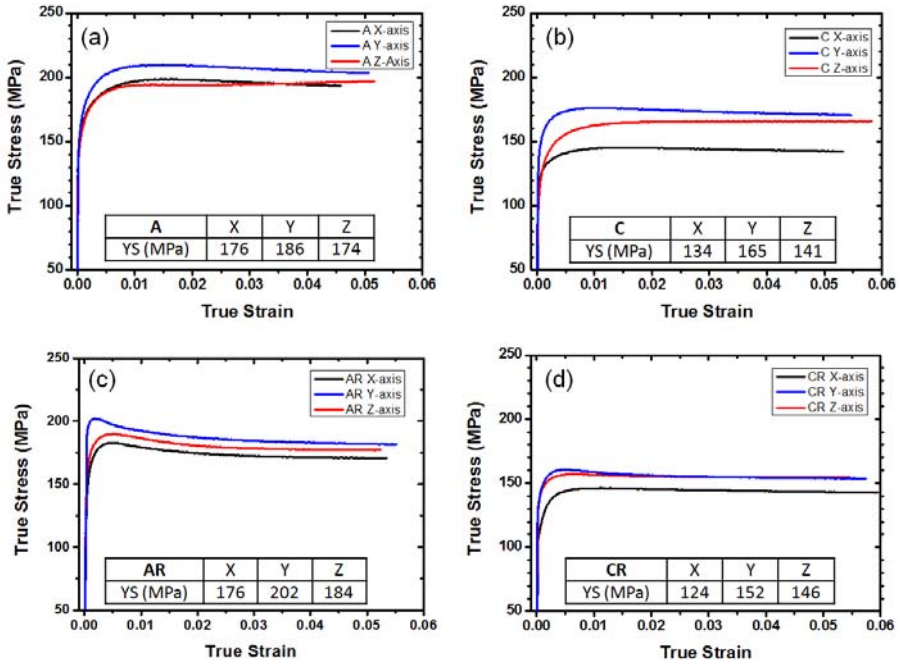

Figure 4. Compressive true stress-strain curves for specimens, (a) A, (b) C, (c) AR and (d) CR, deformed along three orthogonal directions.

3.3. Shear bands

After compression tests, the as-ECAE specimens show a uniform distribution of fine slip traces, while the annealed specimens exhibit distinct bands of flow localization (shear bands). The appearance of shear bands in the annealed specimens also depends on the processing route and the loading direction. Both the AR and CR specimens have similar orientations of shear bands with respect to the loading

direction, but the shear bands are fainter in specimen CR. Specimen AR compressed along the *X*-direction only exhibits one set of shear bands on the Z-plane, which is parallel to the *Y*-axis, while two sets of shear bands are aligned at angles of approximately ±45° to the *X*-axis on the *Y*-plane (figure 5a). Two sets of shear bands aligned at approximately ±45° to the *Y*-axis were observed on the *X*-plane when the specimens were compressed along *Y*-axis (figure 5b and 5c). However, there is only one set of shear bands observed on the *Z*-plane in specimens compressed along the *Y*-direction, which is approximately parallel to the *X*-axis (figure 5b). For specimens compressed along the *Z*-axis, weak signs of shear bands are observed, which can be better described as a distribution of fine slip lines.

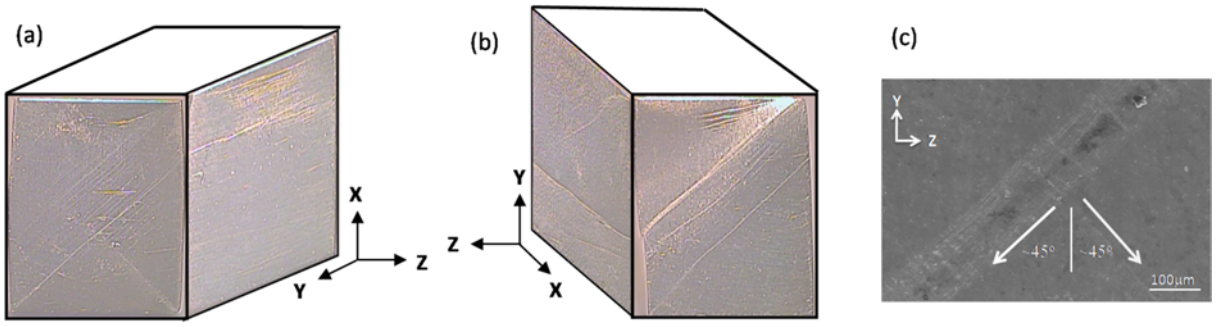

Figure 5. Micrographs showing shear bands on the sample surfaces after compression tests in the AR specimen. (a) Optical micrograph of the Y- and Z- planes of specimen compressed along X-axis, (b) optical micrograph of the X- and Z- planes of the specimen compressed along the Y-axis, and (c) SEM micrograph showing two sets of shear bands on the X-plane of specimen compressed along the Y-axis.

4. Discussion

4.1. Effect of ECAE route (strain-path change) and annealing on the compression behavior

The occurrence of higher yield and flow stresses in specimen A than C is attributed to the smaller grain size and higher proportion of HABs in specimen A. Metals with smaller grain sizes are considered to have higher strength according to the Hall-Petch relationship. However, the grain size effect was found to contribute only 5 MPa to yield stress in A and C specimens from the Hall-Petch slope in this aluminum [8]. The difference in yield stress between samples A and C far surpasses 5 MPa. It is therefore suggested that boundary structure in addition to grain size has a considerable contribution to the strength of this UFG aluminum. Specimen C consists of mainly LABs, which are weaker barriers to dislocation propagation, and consequently result in lower yield stress.

Several factors can affect the anisotropic mechanical response of aluminum, such as texture, grain boundary structure and grain shape. The textures of the two specimens are found to be similar [22] and therefore, the cause of texture can be excluded. The directionality in microstructure might be another possible cause responsible for the anisotropic mechanical behavior. Specimen C has more equiaxed grains surrounded by mainly LABs and some randomly distributed HABs, while specimen A has elongated grains with high proportion of HABs, which are aligned mainly along the X-axis. If the aforementioned factor is the major cause for the anisotropic mechanical response, specimen A should have more pronounced directionality in mechanical behavior. However, the anisotropic behavior is more evident in specimen C. Thus, this proposition could also be ruled out. In mechanical testing, ECAE specimens experience a strain-path change with respect to the previous strain imposed in the ECAE process. It is possible that the anisotropic flow responses could be related to this strain-path change [17, 19]. A more detailed discussion is given in section 4.2.

The occurrence of yielding peak is attributed to the shortage of mobile dislocations, which in turn requires a higher dislocation velocity to satisfy the applied strain rate [25]. It has been shown that UFG aluminum with smaller sizes and low dislocation densities [8] exhibits a significant yielding peak

phenomenon. The absence of yielding peaks on the as-ECAE specimens indicates the existence of sufficient mobile dislocations. However, the annealed specimens, AR and CR, exhibit yielding peaks. From the microstructural examinations of the AR and CR specimens, the diffraction contrast is observed to be more uniform than in the as-ECAE state, A and C specimens, indicating defect density and internal stresses are substantially reduced in the annealed state (figures 1 to 3). Therefore, a high dislocation velocity is required to fulfil the applied strain rate and results in yielding peak [8, 25].

4.2. Relation between plastic anisotropy and the shear patterns in ECAE

Shear bands are observed in the annealed specimens in conjunction with the presence of yielding peaks (figure 5). Shear banding is a common feature in UFG metals during mechanical testing, both tensile and compressive, and result from flow localization [8, 26]. The development of shear bands in UFG metals can be related to its inherent low work-hardening rate. Low temperature annealing can only cause partial recovery of the dislocation structure produced by ECAE. The following shear deformation imposed in ECAE can still affect anisotropic flow localization in the annealed specimens.

A shear strain ε_{XZ} is imposed in each ECAE pass to the material. In route A, deformation occurs on two slip planes alternately in consecutive passes, while in route C deformation occurs on one shear plane with opposite shear direction in consecutive passes. Shear bands on specimens compressed along the *X*-direction have the same orientations as the shear planes in ECAE route A. However, compression along the *X*-direction reverses the stress direction applied during ECAE, and can result in a Bauschinger effect [14] to reduce the yield stress along the *X*-axis. Consequently, the yield stress is the lowest among the three orthogonal directions. Compression along the *Y*-direction results in a shear band orientation distinctly different from the shear planes generated in ECAE, and accordingly, new dislocations driven by different stress components need to be activated and a higher flow stress is required. This results in the highest yield/flow stress in the *Y*-axis among the three directions, an effect of strain path-change suggested by Beyerlein *et al.* [19]. For specimens compressed along the *Z*-axis, the maximum shear stress occurs on the same shear plane and direction as those operated in ECAE, and therefore, the yield stress is intermediate among the three orthogonal directions.

The stronger anisotropic response in specimen C compared to A is considered to be related to deformation occurring on single shear plane during the ECAE route C process. The shear direction is continuously reversed on the same shear plane during consecutive extrusions in route C. However, deformation is imposed on two shear planes and four shear directions in the ECAE route A process [21]. It is therefore suggested that during the ECAE process, dislocations on fewer slip systems are activated in route C than in route A. For compression tests along different loading directions of ECAE processed materials, dislocations on different slip systems should be activated to accommodate the applied strain. The characteristics of dislocations introduced in ECAE can affect the mechanical response in post-ECAE loading. Due to the activation of fewer dislocation slip systems in specimen C, a stronger anisotropic mechanical behavior is expected in specimen C than A. The anisotropy in mechanical response is reduced after annealing, which can be ascribed to partial annihilation of the pre-existing dislocations. Specimen CR has fewer activated dislocations left from ECAE and new dislocations are generated during the following compression tests along all three orthogonal directions, resulting in similar yield/flow stresses along the three directions.

5. Conclusions

In this work, the anisotropy of mechanical response of AA1050 processed by ECAE routes A and C has been investigated in the as-processed and recovered conditions. The main results are listed below.

(1) Specimens A and AR exhibit higher strength than specimens C and CR due to the smaller grain size and higher fraction of HABs in specimens A and AR.

(2) Specimens produced by both ECAE routes show qualitatively similar anisotropic responses under compressive loading along the three orthogonal directions of the ECAE billet. The yield stress is the highest in compressive testing along the Y-direction, while the lowest value of yield stress appears in testing along the X-direction. The differences can be related to the effect of strain-path change,

namely that different slip system activities are induced for specimens loaded along different directions with respect to the last ECAE pass.

(3) The plastic anisotropy in specimen A less than that in specimen C. This difference can be explained by the deformation occurring on single shear plane and two shear directions during ECAE route C, while the deformation is imposed on two shear planes and four shear directions in route A. It is then expected that during ECAE process, dislocations on fewer slip systems are activated in route C than in route A. As the characteristics of the dislocations introduced in ECAE may affect the mechanical response in post-ECAE loading then because fewer dislocation slip systems are activated in route C, a stronger anisotropy in mechanical behavior is expected in specimen C than in A.

(4) The plastic anisotropy persists in the annealed specimens, AR and CR, but to a reduced extent. The reduced anisotropy in mechanical response after annealing can be ascribed to the annihilation of pre-existing dislocations resulting from the ECAE process.

(5) Shear bands are observed in annealed specimens in conjunction with the presence of a yielding peak. Both the AR and CR specimens have similar orientations of shear bands with respect to the loading direction, but the shear bands are weaker in the CR specimen.

Acknowledgments
The authors acknowledge the financial support from the National Science Council (NSC) of ROC under contracts NSC 98-2221-E-035-015 and the discussions with Professor Po-We Kao at Department of Materials and Optoelectronic Science, National Sun Yat-sen University.

References

[1] Iwahashi Y, Horita Z, Nemoto M and Langdon TG 1998 *Acta Mater.* **46** 3317
[2] Gholinia A, Prangnell P B and Markushev MV 2000 *Acta Mater.* **48** 1115
[3] Sun P L, Kao P W and Chang C P 2004 *Metall. Mater. Trans.* **35A** 1359
[4] Chang C P, Sun P L and Kao P W 2000 *Acta Mater.* **48** 3377
[5] Humphreys F J, Prangnell P B, Bowen J R, Gholinia A and Harris C 1999 *Phil. Trans. R. Soc. Lond.* **357A** 1663
[6] Yu C Y, Sun P L, Kao P W and Chang C P 2004 *Mater. Sci. Eng.* **A 366** 310
[7] Wang J, Iwahashi Y, Horita Z, Furukawa M, Nemoto M, Valiev R Z and Langdon T G 1996 *Acta Mater.* **44** 2973
[8] Yu C Y, Kao P W and Chang C P 2005 *Acta Mater.* **53** 4019
[9] Hayes R W, Witkin D, Zhou F and Lavernia E J 2004 *Acta Mater.* **52**
[10] Cheng S, Spencer J A and Milligan W W 2003 *Acta Mater.* **51** 4505
[11] Li Y J, Zeng X H and Blum W 2004 *Acta Mater.* **52** 5009
[12] Sun P L, Yu C Y, Kao P W and Chang C P 2005 *Scripta Mater.* **52** 265
[13] Segal V M 1995 *Mater. Sci. Eng.* **A197** 157
[14] Haouaoui M, Karaman I and Maier H J 2006 *Acta Mater.* **54** 5477
[15] Alexander D J and Beyerlein I J 2005 *Mater. Sci. Eng.* **A 410-411** 480
[16] Beyerlein I J, Li S and Alexander D J 2005 *Mater. Sci. Eng.* **A 410-411** 201
[17] Li S 2007 *Scripta Mater.* **56** 445
[18] Horita Z, Fujinami T and Langdon T G 2001 *Mater. Sci. Eng.* **A 318** 34
[19] Beyerlein I J, Alexander D J and Tomé C N 2007 *J. Mater. Sci.* **42** 1733
[20] Xu C, Száraz Z, Trojanová Z, Luká˘ P and Langdon T G 2008 *Mater. Sci. Eng.* **A 497** 206
[21] Zhu Y T and Lowe T C 2000 *Mater. Sci. Eng.* **A 291** 46
[22] Sun P L, Cerreta E K, Bingert J F, Gray III GT and Hundley M F 2007 *Mater. Sci. Eng.* **A 464** 343
[23] Beyerlein I J and Toth L S 2009 *Prog. Mater. Sci.* **54** 427
[24] Kallend J S, Kocks U F, Rollett A D and Wenk H R 1991 *Mater. Sci. Eng.* **A132** 1
[25] Johnston W G and Gilman J J 1959 *J. Appl. Phys.* **30** 129
[26] Yu C Y, Sun P L, Kao P W and Chang C P 2005 *Scripta Mater.* **52** 359